



An experimental study on root-reinforced soil strength via a steel root analogue in unsaturated silty soil

Jiale Zhu¹ · Abbas El-Zein¹ · David W. Airey¹ · Guien Miao¹

Received: 25 February 2022 / Accepted: 25 April 2023 / Published online: 20 June 2023
© The Author(s) 2023

Abstract

Landslides due to catastrophic weather events, especially heavy rainfall, have risen significantly over the last several decades, causing significant damage and affecting the health and livelihoods of millions of people. Using tree roots to bioengineer shallow slopes has been proven to be a cost-effective, sustainable measure and thus has gained increasing popularity. As slope failure often occurs under heavy precipitation, it is important to understand the mechanical interactions in the soil matrix surrounding a root to better estimate the reinforcement capacity of a root system, especially as the soil undergoes wetting from drier conditions. However, very few studies of root reinforcements have considered the effects of degree of saturation on behaviour. In this study, steel wires are used as a root analogue to explore the impact of root geometry, soil dilation and soil saturation on the pull-out behaviour of a root and three commonly used unsaturated soil strength models have been used to interpret the pull-out results. It was found that roots with larger diameter did not contribute to additional resistance. Also, a linear relationship between degree of saturation and pull-out strength was identified over a large range of suctions and one of the unsaturated soil strength models seemed to provide a more reasonable interpretation. The results will help future bioengineering slope design by improving the understanding of soil-root interface behaviour, including the effect of root diameter in slippage failure and greater emphasis on the importance of taking degree of saturation into account in unsaturated soil strength models.

Keywords Bioengineering slope · Pull-out experiment · Root reinforcement · Root analogue · Unsaturated soil

1 Introduction

Reinforcement with vegetation is an increasingly popular approach to bioengineering slopes due to comparatively low costs, greater potential for conservation and better aesthetics in comparison with traditional slope reinforcement methods. The efficacy of a root system in reinforcing soil is influenced by root properties and soil conditions. The former includes root geometry [18, 29, 52, 70], root tensile strength [42, 44], root hair bonding friction [52] and root spacing [17], while the latter comprises soil saturation [52] and matric suction [36, 41, 48].

Since simple root reinforcement models such as those of Waldron [68] and Wu et al. [71] were first proposed,

predicted strengths have been found to significantly overestimate experimental measurements [44] and this has led to renewed efforts to develop new models. Recent models are frequently based on the fibre bundle model (FBM) with roots [45] which assumes that the strength of reinforced soil depends almost entirely on root properties. All fibre bundle models assume an ultimate breakage failure for the individual roots in a bundle but differ in the load-sharing mechanism [38]. Hence, the root system's predicted strength is mainly a function of the tensile strength of the roots. Soil conditions, especially the effect of matric suction, which greatly affects soil strength, are acknowledged as important, or potentially important [37, 45, 48, 52, 75] but have rarely been taken into account in root reinforcement models. Work incorporating unsaturated soil response in root-reinforcement behaviour include Schwarz et al. [52], which was one of the first attempts at incorporating the influence of matric suction in root reinforcement, but only assumed a linear relationship between degree of

✉ Jiale Zhu
jiale.zhu@sydney.edu.au

¹ The University of Sydney, Zetland, Australia

saturation and matric suction. Another example is the work of Kamchoom et al.'s [30] which used an unsaturated strength model from Khalili and Khabbaz [31] to back-calculate the coefficient of lateral earth pressure when interpreting results from a pull-out test for a root analogue. Mahannopkul and Jotisankasa [36] applied the independent stress variable approach [15] in interpreting the results of a direct shear box test on root-reinforced soil.

Vegetation influences soil strength by altering soil properties as root systems can lower the moisture content in the soil via transpiration [42]. Therefore, soil moisture content will affect the performance of root reinforcement. In-situ shear tests have shown significant improvements in the shear strength of unsaturated root-soil systems as compared to saturated system [12, 26, 74]. Furthermore, laboratory experiments have shown that the moisture content can affect root mechanical behaviour [17, 75]. The effects of moisture content on pull-out capacity have been studied extensively for piles [66, 67], soil nails [19, 20, 57, 73] and geotextiles [24, 25]. On the other hand, studies have only recently [21, 30, 41, 54, 59, 69, 75] examined this effect in the case of roots or analogues. These studies have found that existing root reinforcement models are often based upon data that does not take the soil moisture state into account or assumes the simplest relationship regardless of the condition of the soil and there is little comparison of the applicability of different models.

Experimental studies of other geo-reinforcement materials have shown the importance of unsaturated soil conditions in reinforcement behaviour [20, 24, 57, 67]. Table 1 summarises studies on various types of geo-reinforcement

material in unsaturated soils. In these materials, slippage failure occurs at the soil-reinforcement interface. Su et al. [57] conducted soil nail pull-out experiments with completely decomposed granite under degrees of saturation ranging from 37.83 to 99.57% and various vertical pressures. Their results show a non-monotonic relationship between peak pull-out shear resistance and degree of saturation, under the same vertical pressure, with variability of up to 250% in peak resistance within the studied range of degrees of saturation. Similarly, Gurpersaud et al. [20] found the peak pull-out stress for a pile in unsaturated poorly graded sand to be almost double its equivalent in saturated sand. Kamchoom et al. [30] conducted vertical pull-out tests with a suction-controlled root analogue made of cellulose acetate and found the peak pull-out resistance was around 37.5% higher in unsaturated silty sand (suction around 25 kPa) than for the saturated case. Moreover, Zhang et al. [75] found that, as the moisture content increases, the root system tended to slip rather than break and so root-soil interface properties became increasingly important in the prediction of the system's strength. It is hence evident that greater understanding of pull-out behaviour in an unsaturated soil can better explain slippage behaviour of root systems. However, many other root-soil studies have not measured the saturation level, which makes it difficult to make comparisons between different studies.

The aim of this paper is twofold. Firstly, it investigates the importance of diameter, soil degree of saturation and soil dilation as factors that affect the mechanical behaviour of root pull-out via experiments using a steel analogue in

Table 1 Literature on pull-out behaviour of various types of geo-reinforcement in unsaturated soil

| Geo-reinforcement | Author | Soil | Nominal dimensions of geo-reinforcement | Peak displacement (mm) | Peak stress (kPa) |
|-----------------------------------|--|-------------------------------|---|------------------------|-------------------|
| Soil Nail | Gurpersaud et al., 2013 | Poorly graded sand | 0.1 m diameter | ~ 2 | ~ 7.9–14.3 |
| | Su et al., 2007 | Decomposed granite fill | 0.1 m diameter | 10–60 | 40–110 |
| | Su et al., 2008 | Decomposed granite fill | 0.1 m diameter | 10–40 | 40–90 |
| Geotextile | Hatami et al. 2008 | Natural fine-grained soil | 0.1 m diameter | ~ 1 | 50–125 |
| | Hatami & Esmaili, 2015 | Minco silt (CL–ML) | 0.06 m*0.06 m | ~ 1 | 4.6–23.2 |
| | Hatami & Esmaili, 2015 | Chickasha clay (CL) | 0.06 m*0.06 m | ~ 1 | 40.6–83.8 |
| Spectra fibre (Root analogue) | Galpathage, 2017 | Silty Clay (CL–ML) | 0.004 m–0.008 m | 20–50 | ~ 53–159 |
| Root | Zhang et al., 2020 | Sand | 0.0005 m–0.0015 m diameter | – | ~ 17.5–23.5 |
| Cellulose-acetate (Root analogue) | Kamchoom et al., 2014, Ng et al., 2019 | Completely decomposed granite | 0.006 m–0.09 m diameter | ~ 50 | 1.2–4.8 |

place of a root. Secondly, it assesses the ability of three unsaturated soil strength models to predict experimental data, with focus on slippage failure of the root analogue.

2 Theory of root reinforcement in unsaturated soils

2.1 Root reinforcement theory

Waldron [68] proposed that the total shear strength of a root-soil system (S_r) consists of the strength of the soil ($\tau = \sigma \tan \phi + c$) and the additional strength generated by the presence of root fibres (s_r): $S_r = c + \sigma \tan \phi + s_r$, where c is the apparent cohesion of the soil; σ is the normal stress applied to the soil and ϕ is the soil's friction angle. Wu et al. [71] drew similar conclusions and presented the additional strength s_r in a form which is now commonly known as the Wu-Waldron Model (WWM):

$$S_r = c + \sigma \tan \phi + T_r * \frac{A_R}{A} * (\cos \theta * \tan \phi' + \sin \theta) \quad (1)$$

where T_r is the average root tensile strength, A_R is the cross-sectional area of root, A is the area of plane of shear, $\frac{A_R}{A}$ is root area ratio (RAR), θ is the angle between a deformed root and the plane normal to the shear plane. According to this model, the tensile strength of the roots is the only contributor to the reinforced strength of the system which is assumed to fail due to root breakage, with roots breaking simultaneously.

Several studies have found that WWM predictions produce an overestimation [27, 34, 44, 55]. For example, Hubble and Rutherford [27] found the additional strength from WWM was up to 215% more than in field experiments due to slippage in the shear zone. To address the overestimation, Pollen & Simon [46] introduced progressive failure via the fibre bundle model (FBM) where the loads on individual roots in the bundle were redistributed.

Several variations on the FBM in root reinforcement were explored under different load-sharing mechanism assumptions [28, 38, 51, 62], but these models still consider breakage as the dominant failure mechanism. These variations focus on the failure within the roots and do not adequately consider failure along the soil-root interface. The interfacial failure is more probable when the soil is close to saturation, which is also when slope failure tends to occur under heavy precipitation. In these cases, slippage could be an important failure mechanism and the interfacial bonding strength, which is the pull-out force (F_{po})/embedded surface area, should replace the tensile strength term T_r in Eq. (1).

Bischetti et al. [7] proposed a root reinforcement model for slope stability based on the infinite slope approach [56]

that is suitable for deep-root-trees, for example *Eucalyptus racemose*, *Angophora costata* which are both native and common in New South Wales, Australia. In this model, only slippage was considered and F_{po} was decomposed into two components to calculate the factor of safety.

In summary, the assessment of the ability of roots to reinforce slopes requires knowledge of both anchorage capacity and tensile strength to determine which is critical. Many existing models emphasise the importance of root strength, but assume little effect from the frictional resistance between roots and soil.

2.2 Soil strength and pull-out capacity in unsaturated soil

2.2.1 Effective stress and shear strength in unsaturated soil

Theories describing unsaturated soil behaviour extend Terzaghi's [61] effective stress framework for saturated soils. Two key approaches are the Bishop and Blight [9] stress framework [3, 31, 35, 53] and the Fredlund et al. [13] independent stress framework [15, 65]. Next, the utility of the Fredlund et al. [15], Khalili & Khabbaz [31] and Lu et al. [35] models in describing the pull-out behaviour are explored.

2.2.2 Bishop's stress variable framework

Bishop and Blight [9] have shown that strength calculations based on effective stress can be used for soils with a degree of saturation above a critical value (e.g. 50% for silts). Bishop [8] proposed the following definition for the effective stress:

$$\sigma' = (\sigma_n - u_a) + \chi(u_a - u_w) \quad (2)$$

where σ_n is the normal stress, u_a is the air pressure and often taken as zero for atmospheric pressure, u_w is the matric suction and χ is a parameter related to water content within soil.

Öberg and Sällfors [43] assumed $\chi = S_r$, where S_r is the degree of saturation which is defined as the ratio of the volume of water to the volume of voids. This assumption is still widely used due to its simplicity and ability to yield reasonable results near saturation. Using this assumption Lu et al. [35] proposed a closed form equation for effective stress in combination with the modified Van Genuchten [63] soil water characteristic curve (SWCC) model, resulting in:

$$\chi = \frac{1}{(1 + [\alpha(u_a - u_w)^n])^{(n-1)/n}} \text{ for } u_a - u_w \geq 0 \quad (3)$$

$$\chi = 1 \text{ for } u_a - u_w \leq 0$$

This expression links effective stress (and subsequently shear strength via the Mohr–Coulomb failure criterion) directly to suctions instead of degree of saturation, which allows consideration of the thermodynamics and places itself within the framework of continuum mechanics [35].

As the assumption of $\chi = S_r$ did not agree with their experimental data, Khalili and Khabbaz [31] proposed an alternative expression for χ which introduced a suction ratio:

$$\chi = 1 \quad (u_a - u_w) \leq (u_a - u_w)_b$$

$$\chi = \left[\frac{(u_a - u_w)}{(u_a - u_w)_b} \right]^{-0.55} \quad (u_a - u_w) \geq (u_a - u_w)_b \quad (4)$$

where $(u_a - u_w)_b$ is the air-entry value.

Although the formulation for χ may vary the shear strength may be determined, knowing the effective stress, using the same expression as for saturated soil, that is

$$\tau = c' + \sigma' \tan \phi' \quad (5)$$

2.2.3 Fredlund independent stress variables

Fredlund et al. [13] calculated the shear strength in unsaturated soil using the following equation:

$$\tau = c + (\sigma_n - u_a) \tan \phi + (u_a - u_w) \tan \phi^b \quad (6)$$

where $\tan \phi^b = \chi \tan \phi$ and ϕ^b is the modified friction angle accounting for the effect of matric suction and can itself be a function of other variables. Fredlund et al. [15] introduced a fitting parameter, κ that is related to the SWCC and can be estimated from the plasticity index [16, 64], and leads to the relation

$$\chi = S_r^\kappa \quad (7)$$

Vanapalli and Fredlund [64] showed that this method yielded reasonable predictions in fine-grained material.

2.2.4 Pull-out capacity in unsaturated soil

The pull-out force can be expressed as

$$F = \pi D \int_0^L \tau dl \quad (8)$$

where τ is defined as in Eqs. (5 or 6), L is the length of embedded root and D is the diameter of the root. In general, the limiting shear stress will vary along the root, but in this study the net stress and suction were kept constant by placing the roots horizontally and the stress is expected to be uniform along the length. Hence, Eq. (8) can be written as:

$$F = \pi DL\tau \quad (8a)$$

Following critical state soil mechanics [5], the soil is considered as a purely frictional material and the cohesion $c = c' = 0$. It is often assumed that ϕ in Equation 6 is equivalent to ϕ' where the effect of dilation, described by a dilation angle (ψ), can be added to the critical state friction angle (ϕ'_{cs}) so that at failure the peak friction angle (within soil) $\phi' = \phi'_{pk} = \phi'_{cs} + \psi$ [5]. It is also commonly assumed that the air pressure is equal to atmospheric pressure, $u_a = 0$ and this enables Eq. (5) to be rewritten as

$$\tau = (\sigma_n - \chi u_w) \times \tan \phi' \quad (9)$$

Vanapalli et al. [67] and Gurbarsud et al. [20] followed the Fredlund independent variable approach and proposed that the pull-out stress can be estimated with

$$\tau = (\tau_{\text{net normal stress}} + \tau_{\text{matric suction}}) \quad (10)$$

where $\tau_{\text{net normal stress}}$ is the pull-out stress contributed by normal stress, $\tau_{\text{matric suction}}$ is the additional strength from matric suction, D and L are as defined previously. The additional strength from matric suction can be expressed in conjunction with Eq. (6) as $\tau_{\text{matric suction}} = -\chi u_w \tan \phi'$, which yields

$$\tau = \sigma_n \tan \phi' - \chi u_w \tan \phi' \quad (11)$$

It can be seen that Eqs. (9 and 11) are mathematically equivalent and this allows comparison of the pull-out force and its components between the two frameworks.

This analysis has assumed that the full frictional resistance of the soil can be mobilised along the root. However, many studies have shown that the friction between soil and inclusions of various kinds is generally less than the soil frictional resistance and depends on both soil properties and the roughness of the root-soil interface. The effect of the interface can be quantified by an interfacial friction angle (δ) that is related to surface roughness, the grain-size, and the dry density of soil [58]. For example, in the case of a steel-silty clay interface for which $\phi < 40^\circ$ [2], δ may be taken as $\delta = \frac{4}{3}(\phi - 14.5^\circ)$. In these studies, the friction angle ϕ accounts for any dilation effects so that the interfacial angle equals to the observed peak friction angle ($\phi^p = \delta^p$). δ^p can be used in lieu of ϕ' in Eqs. (10 or 11) to relate soil shear stress with pull-out stress. Based on Eq. (9 and 11) and the above-mentioned assumptions, the expression of pull-out force at peak can be expressed as

$$F_{po} = (\sigma_n - \chi u_w) \times \tan \delta^p \times \pi DL \quad (12)$$

where F_{po} is the peak pull-out force, δ^p is the interfacial peak friction angle (peak friction angle). The predicted pull-out strengths from the three unsaturated soil strength models differ as a consequence of different formulations for χ . It is worth noting that Khalili and Khabbaz [31] and

Lu et al. [35] adopted the SWCC formulation from Van Genuchten [63] in their models whilst, for the Fredlund et al. [15] model, the SWCC formulation is based on Fredlund and Xing [14]. However, these two different formulations of SWCC have minimal impact on the suction value prediction as both methods provide similar fits to the measured data. Rather, it is the difference in definition of χ between the three models that is expected to make a difference to prediction of peak pull-out force.

In this paper, pull-out capacity calculation combined with three commonly used unsaturated soil strength models are compared using experimental results from pull-out tests, in which a steel wire is used as a root analogue in a high-plasticity silt. A series of factors that could mechanically affect the pull-out capacity of the root are also explored.

3 Materials and methods

3.1 Material

A high-plasticity silt was extracted from a minor landslide site at Charlestown in south Newcastle, New South Wales. Table 2 summarises the key parameters of the soil. The grading of the soil was determined using a Mastersizer 2000 and is shown in Fig. 1. The gravimetric water content (GWC) is defined as $GWC = m_{\text{water}}/m_{\text{soil}}$ where m_{water} is the mass of water and m_{soil} is the mass of dry soil. The volumetric water content (VWC) is defined as $VWC = V_{\text{water}}/V_{\text{soil}}$ where V_{water} is the volume of water and V_{soil} is the total volume of soil.

A dry density of 1.5 g/cm^3 ($e = 0.88$) was selected for the pull-out tests in this study, based on 95% of maximum dry density from a standard proctor compaction test

(ASTM D698). The chosen dry density was at the upper end of the field values at the sampling location, which varied from 1.2 to 1.5 g/cm^3 . It was chosen to ensure a good contact between the wires and the soil while maintaining applicability to the field. Similar levels of compaction have been used in geo-reinforcement testing (e.g. Su et al. [57]) and in previous root analogue testing (e.g. Kamchoom et al. [30]). High dry densities can inhibit root growth, but it is not uncommon to find field densities of 95% of standard, for instance, in roadside compacted clayey soils subject to wetting and drying [32, 33].

The friction angle of soil was determined from a direct shear box test (AS 1289.6.2.2) under saturated condition and the water characteristic curve was obtained via a modified contact filter paper method (based on ASTM D5298). In the filter paper test, the samples were mixed from dry states and compacted in two layers in a 37 mm PVC ring with the filter paper in between. The ring was then sealed and stored at room temperature (around $21 \text{ }^\circ\text{C}$) for two weeks to reach equilibrium. The procedure in the filter paper test was similar to the preparation method of the soil for the pull-out tests, with samples compacted to the same dry density and moisture content as the pull-out tests. Additional points with different moisture content were measured to complete the curve. The measured curve was neither a drying nor a wetting curve (closest to a wetting curve), but the suction, moisture content relation produced was representative of the experiments. A WP4C Dewpoint Potentiometer (measuring total suction in accordance with ASTM D6836) was used to confirm filter paper results in the high suction range where the values of total suction and matric suction converge in a high-plasticity soil [4].

The experimental moisture content, suction data have been input into SOILVISION to obtain a mathematical relationship. The SWCC model proposed by Van Genuchten [63] was found to fit the experimental water content and suction relationship data. The model is often simplified to the following equation [40]:

$$S_e = \left\{ \frac{1}{1 + [\alpha(u_a - u_w)]^n} \right\}^{1-1/n} \quad (13)$$

where S_e is the effective saturation (or the degree of saturation if the residual water content is close to 0), u_a is the air pressure, u_w is the pore water pressure, α and n are soil parameters that are related to air entry value and pore size distribution, respectively.

Another SWCC equation was proposed by Fredlund and Xing [14]:

Table 2 Properties of Charlestown site soil

| Parameters | Unit | Value |
|--|-----------------------|-------------------------|
| In-situ GWC | % | 16 |
| Specific gravity, Gs (ASTM D854—14.) | | 2.82 |
| Maximum Dry Density | g/ cm ³ | 1.56 |
| Optimum GWC, OMC (ASTM D698) | % | 20.5 |
| Plastic limit, PL | % | 31.8 |
| Liquid limit, LL | % | 62.3 |
| Critical state friction angle, ϕ_{cs} | ° | 24.4 |
| USCS standard classification | | High plasticity silt |

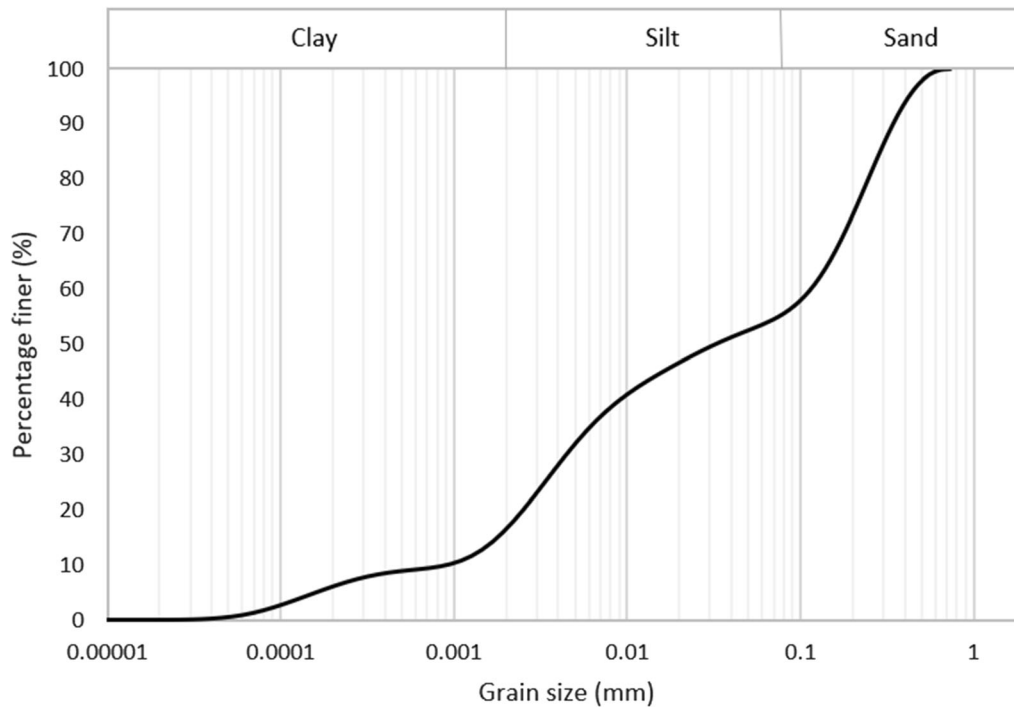


Fig. 1 Particle size distribution from laser diffraction particle size analyser

$$w = w_s \left[1 - \frac{\ln \left[1 + \frac{(u_a - u_w)}{h_r} \right]}{\ln \left[1 + \frac{10^6}{h_r} \right]} \right] \times \left[\frac{1}{\ln \left[e + \left(\frac{u_a - u_w}{a_f} \right)^{n_f} \right]^{m_f}} \right] \quad (14)$$

where w_w is the gravimetric water content, w_s is the saturated gravimetric water content, a_f is a parameter related to the air-entry value, n_f is a parameter related to the rate of water extraction from soil after air entry, m_f is a parameter related to the residual water content and h_r is the suction at which residual water content occurs. This equation was used for Fredlund et al.'s [15] model as shown in Eq. (5). In determining the fitting parameters for the Van Genuchten [63] and on Fredlund and Xing's [14] models, the saturated GWC was calculated to be 31.4% at a void ratio

Table 3 Fitting parameters from the two models

| Parameter | Fredlund and Xing | | Parameter | Value | Unit |
|-----------|-------------------|-------|-----------|----------|------|
| | Value | Unit | | | |
| α | 0.0026 | 1/kPa | a_f | 533.2637 | kPa |
| n | 1.4416 | | n_f | 1.1438 | |
| | | | m_f | 0.9677 | |
| | | | h_r | 8340.29 | kPa |

of 0.88. The air entry value was 128 kPa for both models and the residual volumetric water contents and goodness-of-fit were 0.11%, $R^2 = 0.8715$ and 15.4%, $R^2 = 0.8736$, respectively. The fitting parameters associated with these models are shown in Table 3. Both methods produced similar fitting for the experimental data as shown in Fig. 2.

It might be argued that the soil in this study shows a grain-size distribution with bimodal characteristic, which may cause bimodal behaviour in the SWCC [47, 49]. However, the current experimental data shows unimodal SWCC behaviour and thus, a bimodal degree of saturation and suction relationship was not considered in this study.

3.2 Pull-out experiments

Existing studies [1, 44, 55] have found different root systems exhibit tensile strengths that depend on species, elasticity, water content, diameter and other factors. Due to a lack of control over properties in real root-soil systems, investigating the effect of root geometry and soil moisture content on the mechanical behaviour under slippage is difficult. In this study, a root was modelled through a steel wire analogue in order to investigate the effect of the root-soil interaction without having to consider root breakage or complex root geometry. Although the behaviour of a steel wire may differ from that of an actual root, the steel wire is still capable of simulating the behaviour of mechanical pull-out. It is geometrically similar to a segment of straight root whilst allowing better control over geometric and

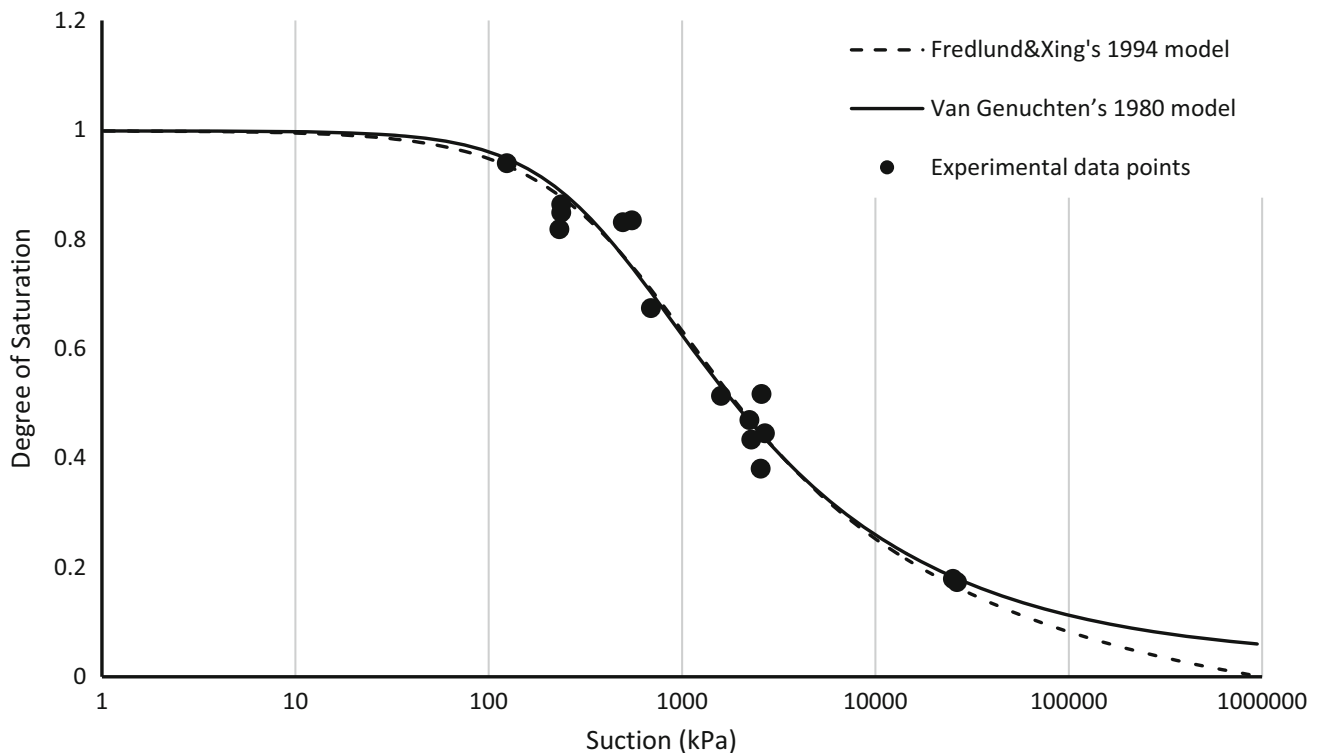


Fig. 2 Degree of saturation and suction relationship of the experimented soil at 1.5 g/cm^3

physical properties. Limitations on selecting root analogues are discussed at the end of the article.

The steel wire analogue used for the experiments consisted of 7 high-grade 304 stainless steel strand each with 7 sub-strands. They had a rougher surface than standard stainless steel bar and thus enhanced interaction between root analogue and soil. The surface roughness of the wire strand was measured with a Hirox digital microscope RH-2000 which yielded an approximate normalised surface roughness $R_n = 30$. R_n is a measure of the relative surface roughness respecting soil particle sizes and follows the definition in Han et al. [23]. The steel wires were embedded in the soil, which was compacted in three layers, at a minimum spacing of 35 mm. They were connected to a bar at three locations shown in Fig. 3b. For different number of wires, they were installed either (a) in the middle if 1 wire was used, (b) at both ends if 2 wires were used, or (c) at both middle and both ends if 3 wires were used. The embedded length of each wire was 285 mm and the wires were pulled out at 0.014 mm/s based on AS1289.6.2.2:2020. As the pull-out was at a relatively slow speed, the matric suction was considered to be constant throughout the experiment.

The soil was mixed to a target moisture content and sealed for two weeks to reach equilibrium. The soil was compacted into the box in three layers to ensure a uniform compaction as shown in Fig. 3a. Care was taken to ensure

an even distribution of soil and levelled compaction surfaces. The lower two layers were each 20 mm deep. After compaction of the first two layers, the wire(s) were then laid on the soil and attached to the bar before the upper 40 mm-deep layer was compacted on top. An overburden pressure of 22.1 kPa was then applied.

The wire diameter, target moisture content, number of wires were the main variables as shown in Table 4. All of these combinations were tested for soil with 1.5 g/cm^3 dry density. The dry density was also varied to qualitatively explore the effect of dilation. Two 2.5 mm diameter wires, at 16% target moisture content were tested for soil with 0.9 and 1.2 g/cm^3 densities. The pull-out force and displacement of the wires were recorded.

4 Results and discussion

4.1 Pull-out behaviour of analogue

Figure 4 shows a comparison between the pull-out behaviour of the steel root and real roots [17, 50]. The measured pull-out loads were converted into pull-out stress by dividing them by surface area of root in contact with soil. Due to large differences in total pull-out distance, the displacement was also converted to displacement over total displacement. In all three behaviours, the pull-out stress

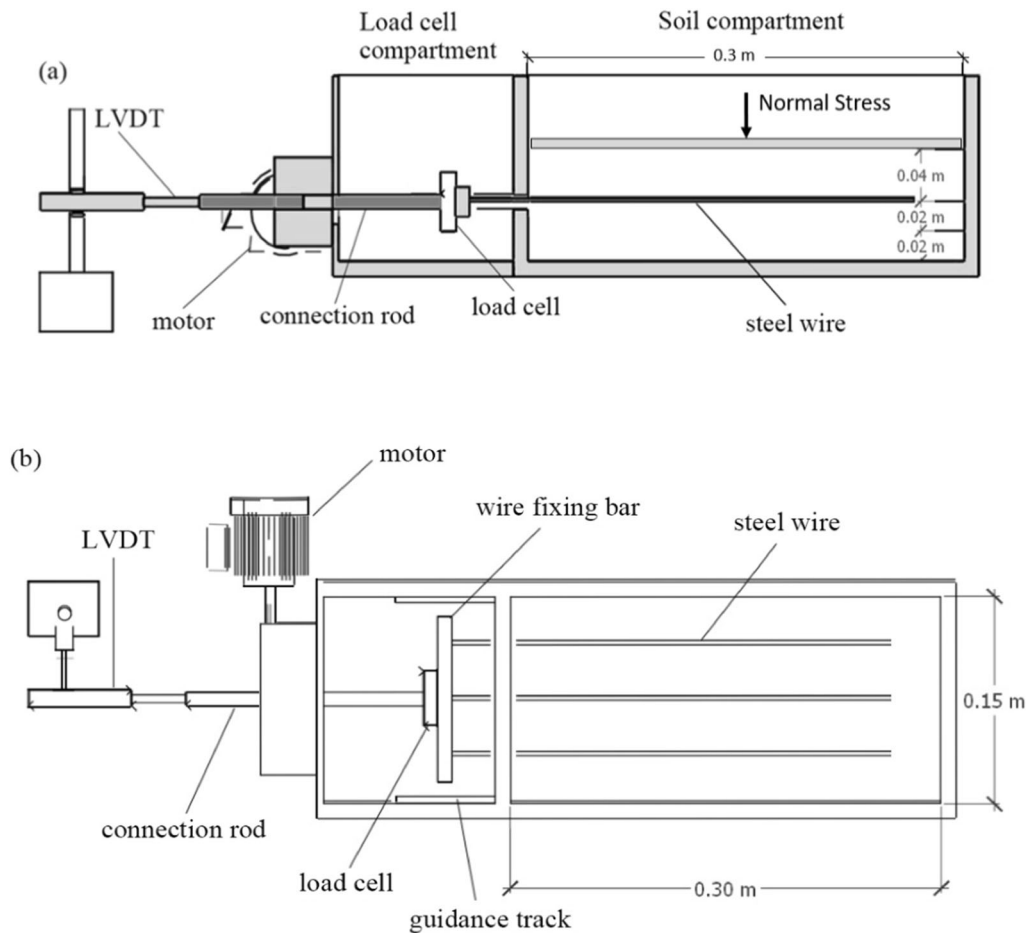


Fig. 3 Schematic drawings of the pull-out box (if three wires used)

Table 4 Variables in the experiment

| Parameter | Unit | Values/Range |
|-------------------------|-------------------|---------------|
| Diameter | mm | 1.5, 2.5, 4.5 |
| Target moisture content | % | 16, 21, 26 |
| Number of wires | | 1, 2, 3 |
| Dry density | g/cm ³ | 0.9, 1.2, 1.5 |

increases rapidly at small displacements and decreases to a constant value at larger displacements. Schwarz et al. [52] noted that the pre-peak behaviour represents the bonded state, where the soil matrix is undisturbed, whereas the residual behaviour represents the de-bonded state, where the soil and the root (analogue) separate, and the root starts to slide within the soil.

Although the overall pattern of the pull-out responses is similar, the peak shear stress is lower and the displacements to the peak are significantly greater for the real roots. As the soil and conditions are not comparable in the other

studies, differences are to be expected. Nevertheless, the smaller displacements to peak for the wires can be explained by their higher stiffness, and their limited extensibility is expected to lead to the peak shear stress being mobilised simultaneously all along the wires making the interpretation of the results straightforward. All in all, the similarity in behaviour provides some support for the use of steel as a root analogue.

4.2 Effect of root diameter and surface area

Figure 5 depicts the pull-out stress range and mean value versus displacement for 27 tests and shows that the peak stress is largely independent of the wire diameter. The low sensitivity of peak stress to diameter shown in Fig. 5a is replicated for different moisture contents as shown in Fig. 5b. Nevertheless, some diameter dependency of the final pull-out stress, particularly for lower GWC levels, has been observed as shown in Fig. 5c.

Figure 5a shows that the increase in diameter tends to prolong the displacement interval over which the peak

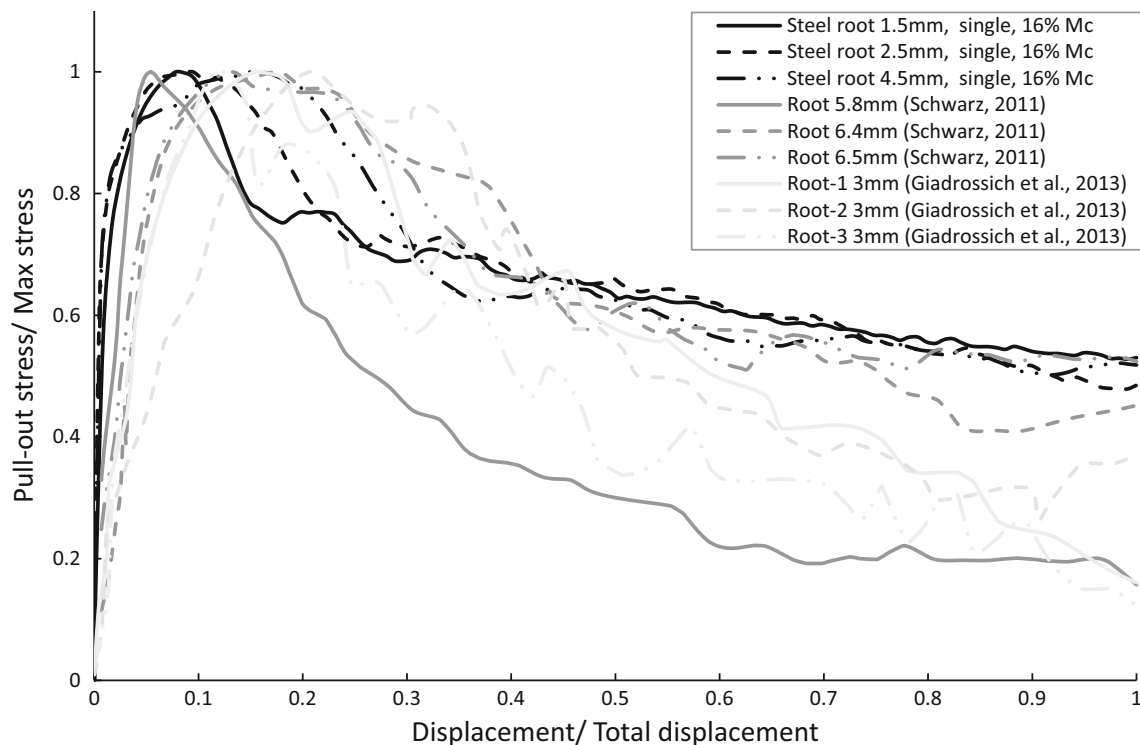


Fig. 4 Experimental results for pull-out behaviour of steel bar compared with real root system [17, 50] with diameter as variable

shear stress occurs. If the first significant point of inflection is defined as the end of initial peak, a clear positive relationship between root diameter and the displacement at which the initial peak ends can be seen in Fig. 6. The three lines of best fit for GWC at 16%, 21% and 26% showed R^2 of 0.9122, 0.8866 and 0.7518, respectively. Similar behaviour has been reported for individual roots by [45, 50, 72] suggesting that failure is associated with larger displacements as the diameter of the embedded root increases.

Results of pull-out experiments with different diameters but similar surface area and moisture content are shown in Fig. 7 (3 wires at 1.5 mm diameter, 2 wires at 2.5 mm diameter and 1 wire at 4.5 mm diameter with respective surface areas of 14.1, 15.8 and 14.9 mm²/mm length). The peak shear stress occurs at a higher displacement for the 4.5 mm diameter wire, than the other two smaller diameters.

Mechanical interactions between roots can decrease the peak shear stress by around 15% [17], because the failure pattern may shift from single-root interfacial failure to bundled-root block failure. However, Fig. 8 shows that the peak pull-out stress is similar in the case of different spacings (represented with number of wires) for 1.5 mm diameter wire. This suggests that these tests were not affected by interactions between wires. Similar results were noted for the data from experiments on 2.5 mm and 4.5 mm diameters. These results indicate that, at the

spacing of 35 mm used in the present experiments, the analogues do not behave as a bundle. This is in line with existing literature [17] showing that bundled interactions occur at spacings of 15 mm but not 35 mm. This indicates that the multiple wires in this study are likely free from the bundle effect and act as independent wires.

4.3 Effect of degree of saturation & soil dilation

A typical set of pull-out-stress curves from tests with a single wire of diameter 4.5 mm, but different moisture contents is shown in Fig. 9. In Fig. 9, all the pull-out stresses rapidly increase to peak and decrease to a relatively stable stress level at a larger displacement. Figure 9 also shows that the peak pull-out stress is higher for soil with lower moisture content.

Figure 10 shows that the degree of saturation has a significant impact on the peak pull-out stress, with a decrease in the degree of saturation associated with higher shear strength. The behaviour appears to be linear, with an R^2 of 0.798. This is in agreement with previous research, also shown in Fig. 10, which depicted a monotonic decrease in pull-out strength with increasing saturation of a flat woven geotextile in Chickasha clay under different overburden pressure [24]. This can be attributed to an increase in soil suctions at lower moisture contents under same dry density, which increases soil resistance.

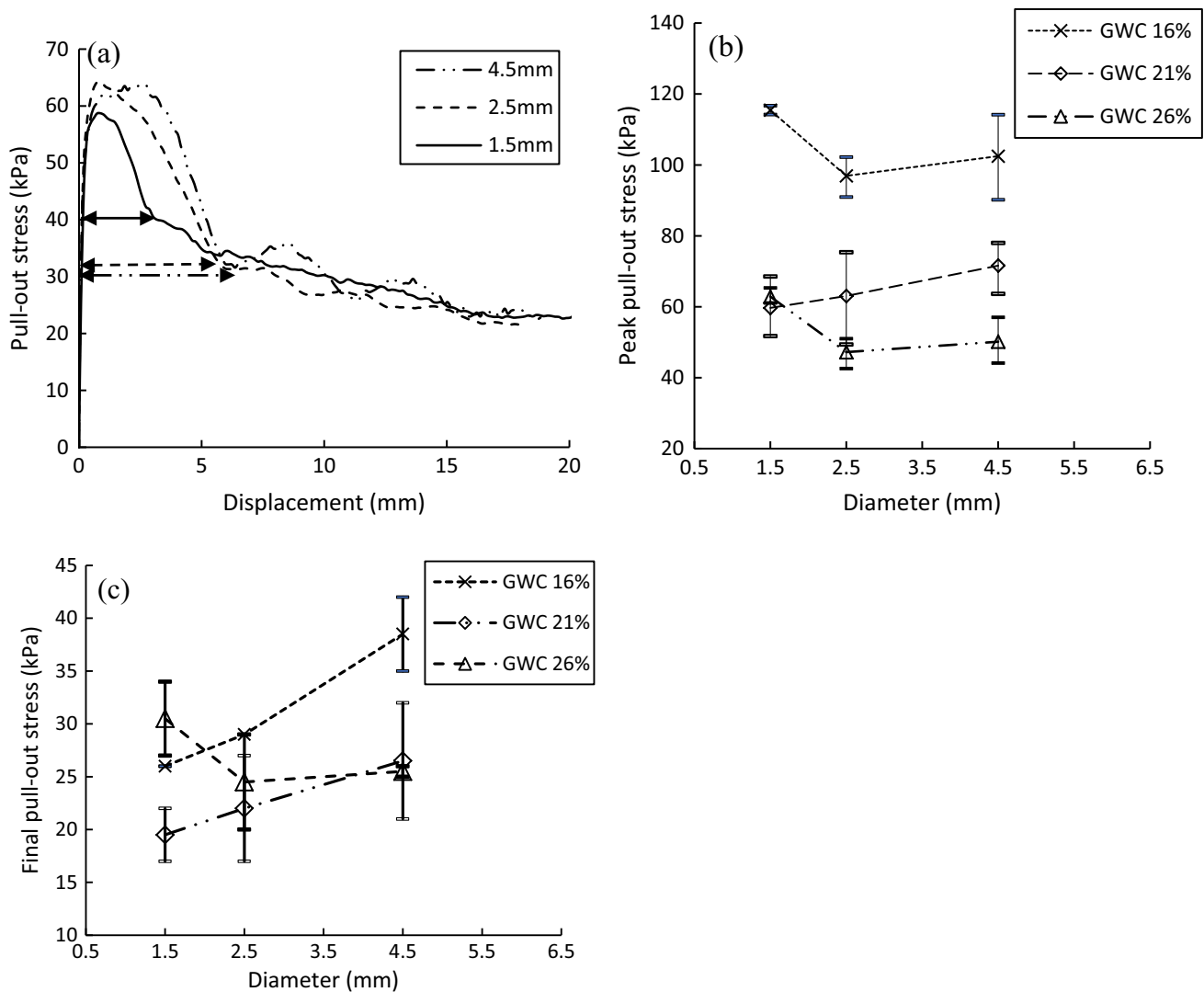


Fig. 5 a Shear stress versus displacement for 3 wires with different diameters at GWC = 21% b measured peak pull-out stress range for different diameters and moisture contents c measured final pull-out stress range for different diameters at moisture contents, the error bars showed the range of measured values and their average

A negative correlation between the final stress and degree of saturation was found in this study, as shown in Fig. 11. Although not negligible, the variation is nevertheless less significant compared to differences in peak pull-out stress. The R^2 based on linear regression analysis was 0.2792. The final stress is only briefly mentioned in previous literature on pull-out tests in various geo-reinforcement structures [20, 25, 39, 67]. Hamid and Miller [22] found through interface shear tests that the final stress was minimally affected by the degree of saturation, which was observed in the pull-out tests of Hatami et al. [25]. But the suction variation range in both materials of these previous studies were relatively small, resulting in a small contribution to the final strength. Suctions for the high plasticity silt in this study ranged from 200 to 2000 kPa are

believed to have resulted in the magnified final pull-out stress for lower degrees of saturation.

The majority of tests in this study were conducted with a dry density of 1.5 g/cm^3 , but a few additional tests were performed at lower dry densities of 0.9 g/cm^3 ($e = 2.1$) and 1.2 g/cm^3 ($e = 1.3$) to explore the effect of dilation. The soil samples were prepared at a constant 16% moisture content at different dry densities producing different degrees of saturation. The results are shown in Fig. 10. It is difficult to draw definitive conclusions from this data because the tests with different densities cover very different suction ranges at same moisture content level. However, based on Fig. 10, it is likely that the decreases in dry density have reduced dilation leading to a decrease in peak shear stress by an amount that is high enough to offset gains in strength due to the increase in degree of saturation.

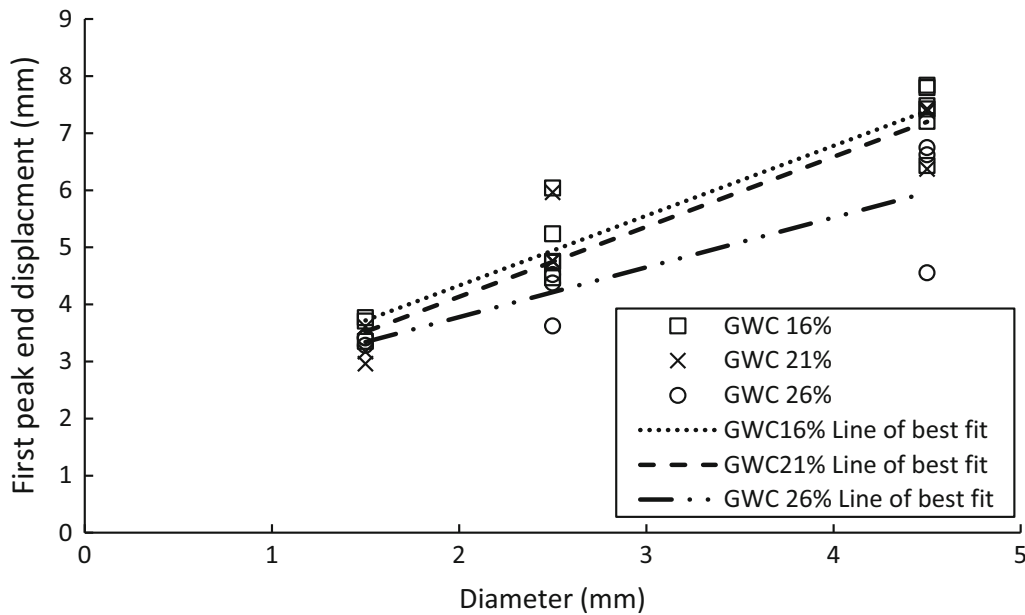


Fig. 6 Displacement of main peak end versus diameter

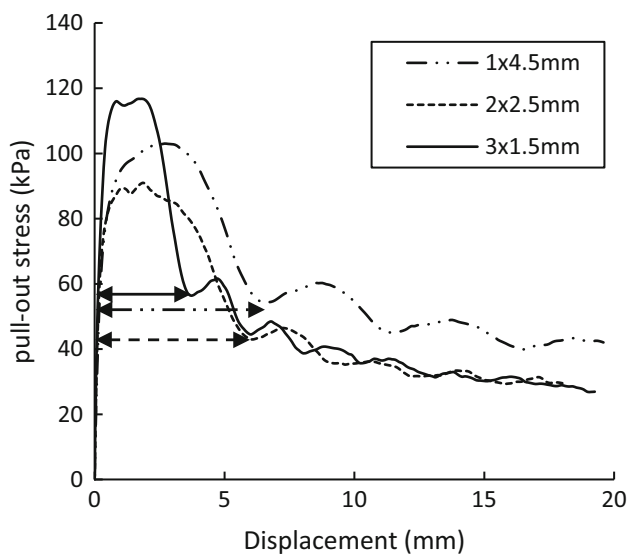


Fig. 7 Peak pull-out stress versus displacement for 3 wires with different diameters but similar total surface areas at $m = 21\%$

This agrees with the finding that, for soils under relatively low normal stresses, the influence of dilatancy is the dominant factor in the soil shear stress [20]. The results suggest that differences in dry density have the potential to significantly affect the pull-out capacity and should be reported in future studies.

4.4 Prediction of unsaturated soil strength equation

The value of δ^p for different suctions was calculated in two steps. First, Eqs. (3, 4 and 7) were used to calculate χ values associated with the SWCC for Lu et al. [35], Khalili and Khabbaz [31] and Fredlund et al. [15] models, respectively. Second, using the calculated χ values and measured F_p values from the pull-out experiments, Eq. (12) yielded an estimate of δ^p . Results are shown in Fig. 12.

It can be seen that Lu et al.’s [35] model, which is essentially letting $\chi = S_r$, generates a δ^p that changes significantly with suction. Fredlund et al.’s [15] model and Khalili and Khabbaz’s [31] model yield relatively stable values of δ^p and give approximately $\delta^p = 8^\circ$ and $\delta^p = 11^\circ$, respectively.

Both calculated values are significantly lower than those angles suggested by existing literature reporting on interfacial angle between a rough steel surface and soil. For example, it has been suggested that the interfacial angle should be taken as 2/3 of the friction angle [61]. In this study, $\phi = \phi'_{cs} = 24.4^\circ$ which gives $\delta = 16.3^\circ$. The chart proposed by Aksoy et al. [2], on the other hand, suggests $\delta = 13.2^\circ$. As both of these values are higher than δ^p , neither value may be appropriate in this study.

To find a more accurate δ , the normalised surface roughness measured was used. According to Han et al. [23], $R_n = 0.3$ would produce a δ/ϕ' of 0.95 and the ratio increases to 1 as R_n increases. This means a $R_n = 30$, which is 100 times larger than the suggested value, would

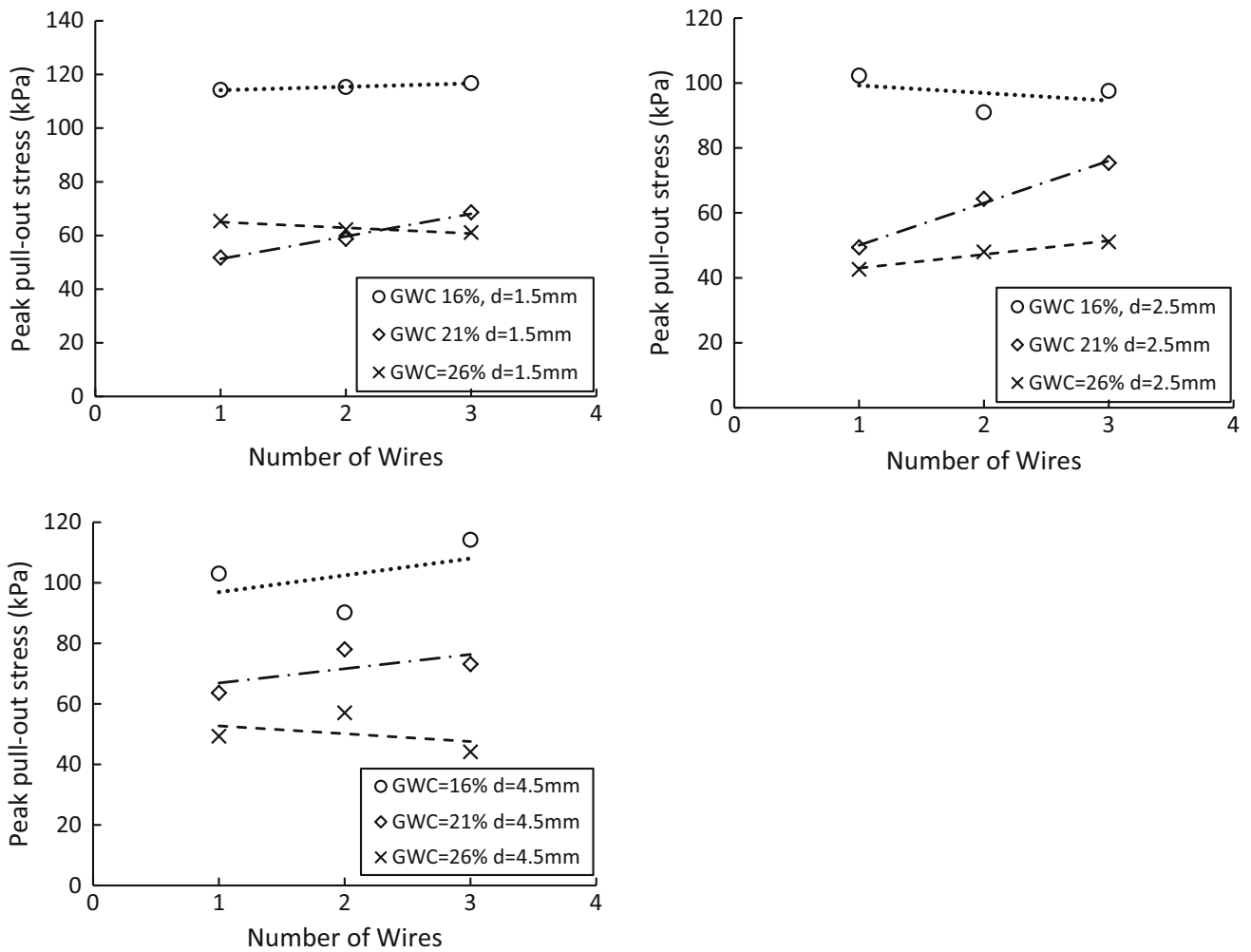


Fig. 8 Peak pull-out stress against different number of wires for different wire groups at various moisture contents

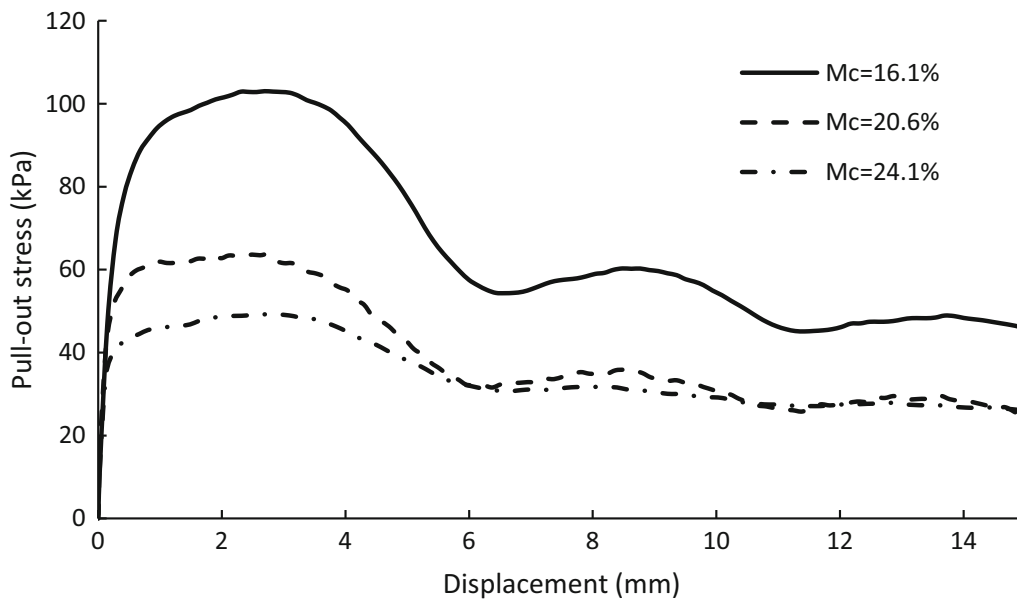


Fig. 9 Pull-out stress versus displacement curve of single 4.5 mm wire under 3 moisture content

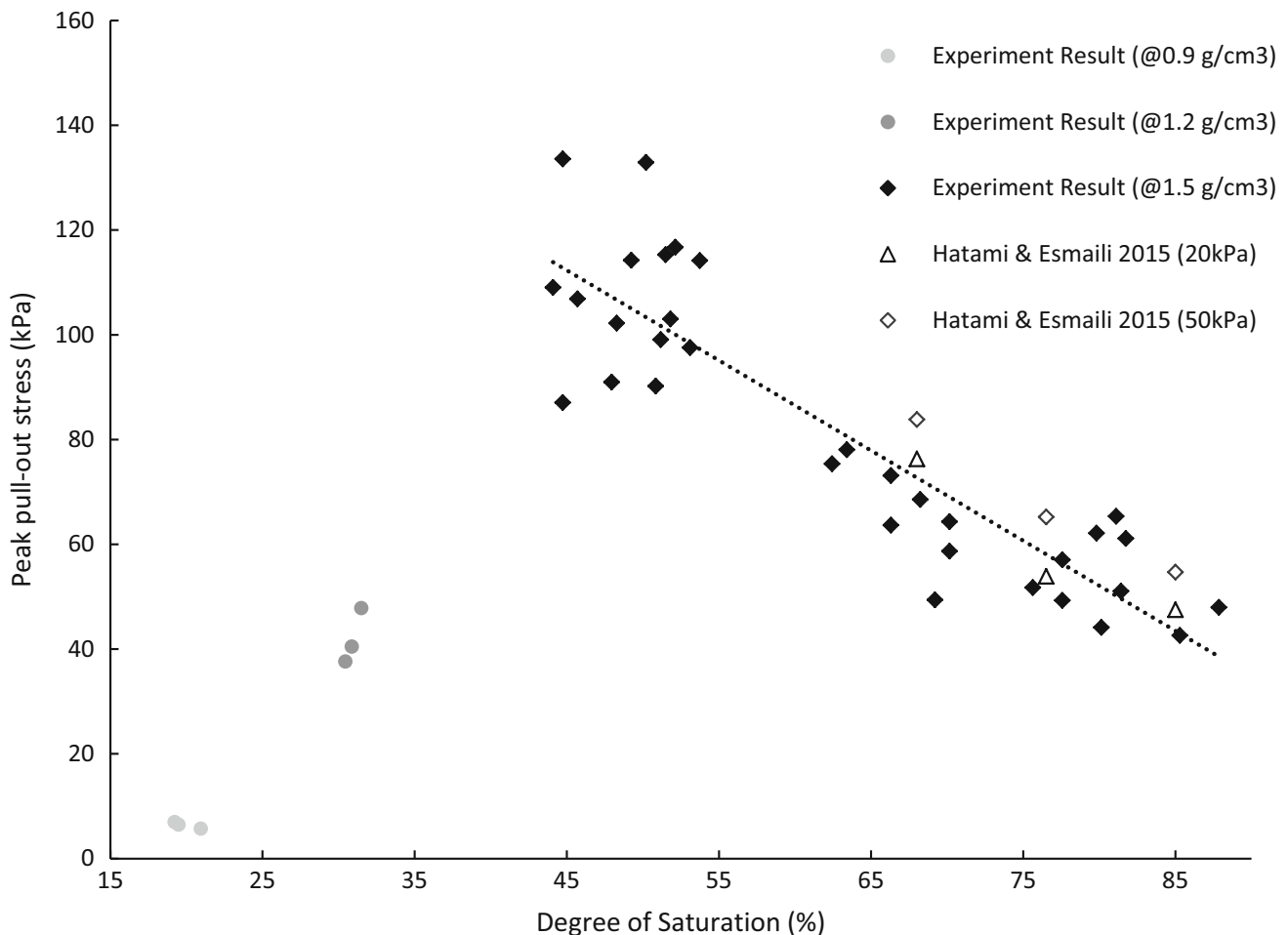


Fig. 10 Peak pull-out stress versus degree of saturation

almost certainly suggest $\delta = \phi'$. However, this does not agree with the experimental observation as little soil was attached to the wire after pull-out and no soil was pulled to the load cell compartment, which indicates that the failure happened between soil-steel interfaces. Such result suggests that the effective contact area between soil and steel may be different and lower than apparent surface area, similar to the concept of the effective unit perimeter [6] in determining the pull-out capacity of geotextiles.

Another explanation for the low inferred friction angle is a result of a potential reduction in effective stress, which could have been caused by a combination of the following reasons. Firstly, shearing of unsaturated soil could have caused the effective stress to reduce as it moves towards a critical state [11]. Secondly, the soil in the narrow shear band surrounding the wire could have experienced a compressive tendency leading to an arching effect during the pull-out. Boulon and Foray [10] suggested that soils surrounding a pile can be modelled approximately by a linear spring in the far-field and this 'spring's' normal stiffness is $K_n = 4G/d$, where G is the soil's shear modulus

and d is the inclusion's diameter. In this study, the densely compacted soil and the small diameter would generate a large normal stiffness and as a result the effective normal stress in the shear zone will be extremely sensitive to displacement. Therefore, a small volumetric strain caused by compressive soil behaviour could have resulted in a significant drop in effective stress. This is the arching effect as Terzaghi [60] first demonstrated, which redistributes the stress applied and can significantly reduce the contact stress. Thirdly, with the local volumetric reduction, the localised void ratio decreases and the localised degree of saturation increases. This would result in a significant decrease in suction and eventually a decrease in effective stress as well.

In this study, the Khalili and Khabbaz's [31] model yields a more stable value of δ^p and, following Milligan & Tei's [39] friction coefficient for mechanical pull-out which represent the ratio between effective friction angle and soil friction angle, this yields:

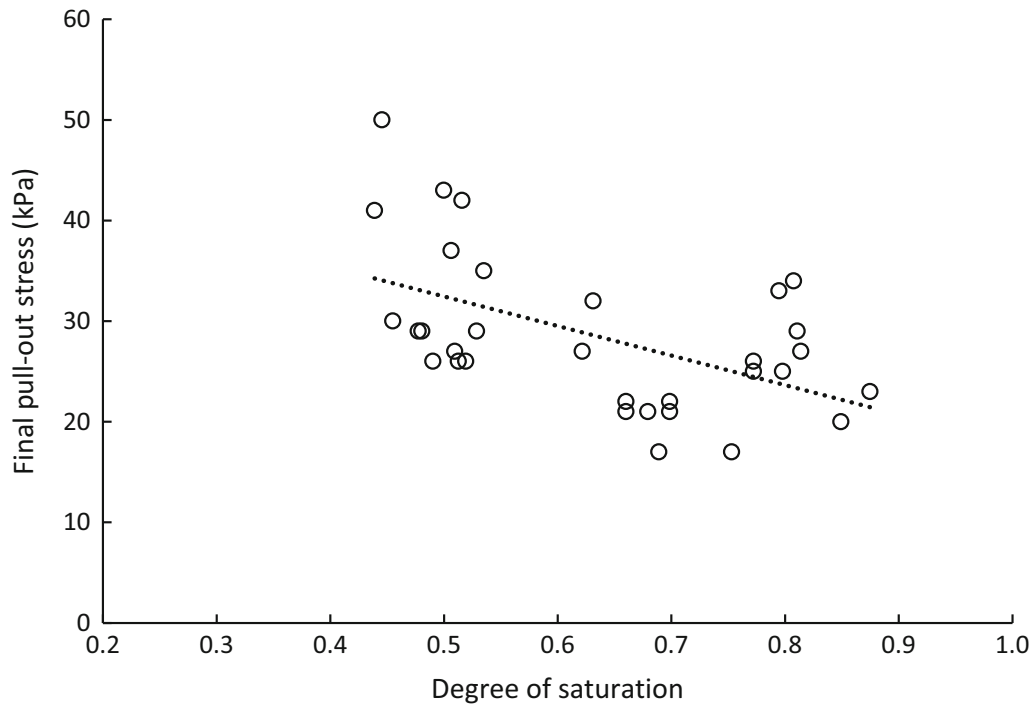


Fig. 11 Final stress versus degree of saturation

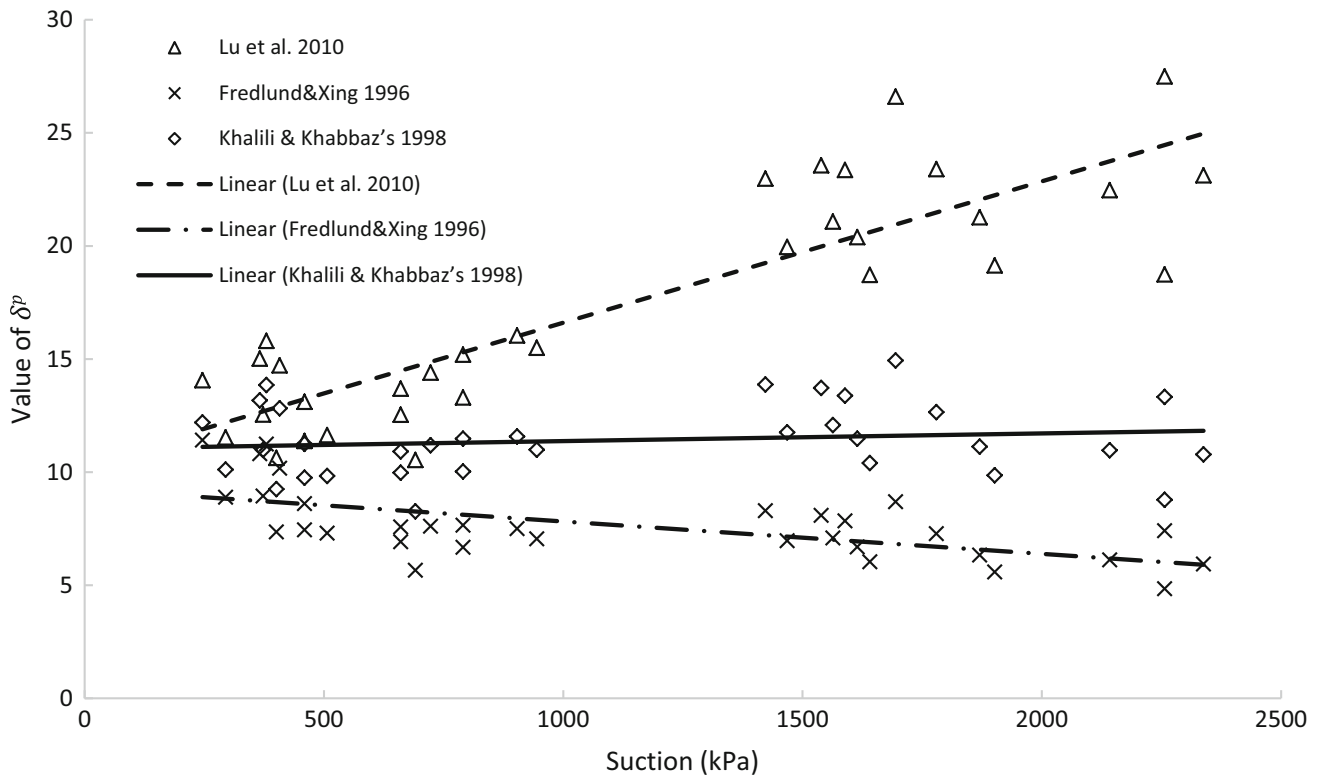


Fig. 12 δ^p versus Suction for 1.5 g/cm^3

$$\mu^* = \frac{\tan \delta^p}{\tan \phi} = 0.428$$

The above approach, applied to peak pull-out stress, was also attempted for the final stress but no model was able to generate a consistent δ value, with larger variation observed over the studied suction range. Nevertheless, the average μ^* can be estimated to be approximately 0.2. A possible explanation for the difference in μ^* at peak pull-out and final stresses proposed by Hamid and Miller [22] is that effect of suction on the final stress is lower than the effect on the peak stress because the menisci between the soil and the interface are disrupted after the peak occurs. As a result, the final stress may depend more on kinetic friction than suctions in the soil, but the degree to which the effect of suctions reduces is still unclear. It is also plausible that the compressive tendency mentioned in the previous section becomes larger and the effective stress further reduces at the final state. This would also result in a much lower μ^* .

In conclusion, no consistent method for the conversion between shear strength in dense unsaturated soil and pull-out stress can be found but relationships have been found between them. In this study, Khalili and Khabbaz's [31] model seems to provide the best means of converting observed peak pull-out stress into an estimate of the effective friction angle.

The experiments are limited in two aspects. Firstly, the use of steel wire as root analogue focuses on the effect of unsaturated soil on root's mechanical behaviour, rather than the root itself. Steel root analogues differ from the real roots mainly by their mechanical properties e.g. tensile strength, surface roughness, elastic modulus and geometry. The most significant difference is the tensile strength which prevents breakage. While this study intentionally focused on slippage behaviour, it should be noted that breakage is still an important factor in root-reinforced soil's failure. From a geometric perspective, the steel wire is used as a simplistic model for straight roots. However, in reality, a significant portion of roots possess a tapered shape and exhibit considerable tortuosity. Future researchers can select different materials (e.g. wooden-filament-3D printed root) to better model root reinforcement behaviour through root analogues. Secondly, the experiment was only conducted in one type of silty soil with a high suction variation. The effect of suction will be smaller in soils that exhibit smaller ranges of suction and future studies using soil with different hydraulic properties are recommended.

5 5. Conclusion

A series of pull-out experiments using steel wire as root analogue was conducted to investigate the impact of variation in root geometry and moisture content on a root's capacity to bio-reinforce soil. Although the tensile strength of the steel is much higher than that of roots and does not allow this study to establish when breakage failure occurs, the results provide insights into likely behaviour of an analogous root under slippage failure. Furthermore, the use of steel wire does not allow for full realistic modelling of the root-soil bond, but the interface behaviour has been quantified in this study through measurement of the surface roughness and the peak friction angle. In future studies, the applicability of the analogue can be further assessed by comparison with real root surface roughness and peak friction angle.

Studying variations of diameter, surface area and spacing (number of wires), moisture content and dry density, the following conclusions can be reached:

- 1) Larger root diameters do not contribute to additional pull-out capacity in cases where the root does not break. However, larger diameters tended to lengthen the peak period of pull-out force which suggests that larger diameter roots may resist pull-out for longer periods during heavy precipitation.
- 2) High dry densities appear to result in significant dilation effects that impact the soil strength.
- 3) A linear relationship between root pull-out strength and unsaturated soil strength has been identified for a material with high suction variation and the results are consistent with previous literature. In this experiment, a very low frictional resistance was inferred. Possible reasons include the geometry of the root analogue, a reduction of effective stress due to shearing of unsaturated soil, compressive soil behaviour leading to arching, or localised change in degree of saturation. More research is needed to explain the exact cause of the low resistance.

The models explored in this study are suitable for slippage failure, which occurs more often in wet soils, and for roots with small diameter and high tensile strengths; however, the models significantly over-estimate the pull-out capacity of root systems. More evidence is required to connect unsaturated soil strength to a prediction of pull-out strength in order to better predict the bio-reinforcement capacity of roots.

Funding Open Access funding enabled and organized by CAUL and its Member Institutions.

Open Access This article is licensed under a Creative Commons Attribution 4.0 International License, which permits use, sharing, adaptation, distribution and reproduction in any medium or format, as long as you give appropriate credit to the original author(s) and the source, provide a link to the Creative Commons licence, and indicate if changes were made. The images or other third party material in this article are included in the article's Creative Commons licence, unless indicated otherwise in a credit line to the material. If material is not included in the article's Creative Commons licence and your intended use is not permitted by statutory regulation or exceeds the permitted use, you will need to obtain permission directly from the copyright holder. To view a copy of this licence, visit <http://creativecommons.org/licenses/by/4.0/>.

References

- Abernethy B, Rutherford I (2001) The distribution and strength of riparian tree roots in relation to riverbank reinforcement. *Hydrol Process* 15:63–79. <https://doi.org/10.1002/hyp.152>
- Aksoy HS, Gör M, Inal E (2018) Determination of friction angles between soil and steel-FRP piles. *Turk J Sci Technol* 13(1):19–23
- Alonso EE, Pereira J-M, Vaunat J, Olivella S (2010) A microstructurally based effective stress for unsaturated soils. *Géotechnique* 60:913–925. <https://doi.org/10.1680/geot.8.P.002>
- Arifin YF, Schanz T (2009) Osmotic suction of highly plastic clays. *Acta Geotech* 4:177–191. <https://doi.org/10.1007/s11440-009-0097-0>
- Atkinson JH (1993) An introduction to the mechanics of soils and foundations: through critical state soil mechanics. McGraw-Hill Book Co., London
- Berg RB, Christopher BR, Naresh CS (2009) Design and construction of mechanically stabilized earth walls and reinforced soil slopes. Federal Highway Administration, Washington, DC
- Bischetti GB, Chiaradia EA, D'Agostino V, Simonato T (2010) Quantifying the effect of brush layering on slope stability. *Ecol Eng* 36:258–264. <https://doi.org/10.1016/j.ecoleng.2009.03.019>
- Bishop A (1959) The principle of effective stress. *Teknisk Ukeblad*
- Bishop AW, Blight GE (1963) Some aspects of effective stress in saturated and partly saturated soils. *Géotechnique* 13:177–197. <https://doi.org/10.1680/geot.1963.13.3.177>
- Boulon M, Foray P (1986) Physical and numerical simulation of lateral shaft friction along offshore piles in sand. pp 127–147
- Burton G, Sheng D, Airey D (2019) Critical state behaviour of an unsaturated high plasticity clay. *Géotechnique* 70:1–34. <https://doi.org/10.1680/jgeot.18.p.178>
- Fan C-C, Su C-F (2008) Role of roots in the shear strength of root-reinforced soils with high moisture content. *Ecol Eng* 33:157–166. <https://doi.org/10.1016/j.ecoleng.2008.02.013>
- Fredlund DG, Morgenstern NR, Widger RA (1978) The shear strength of unsaturated soils. *J Geotech Eng Div* 15:313–321. <https://doi.org/10.1139/t78-029>
- Fredlund DG, Xing A (1994) Equations for the soil-water characteristic curve. *Can Geotech J* 31:521–532. <https://doi.org/10.1139/t94-061>
- Fredlund DG, Xing A, Fredlund MD, Barbour SL (1996) The relationship of the unsaturated soil shear strength to the soil-water characteristic curve. *Can Geotech J*. <https://doi.org/10.1139/t96-065>
- Garven EA, Vanapalli SK (2012) Evaluation of empirical procedures for predicting the shear strength of unsaturated soils. *Unsaturated Soils*. [https://doi.org/10.1061/40802\(189\)219](https://doi.org/10.1061/40802(189)219)
- Giadrossich F, Schwarz M, Cohen D, Preti F, Or D (2013) Mechanical interactions between neighbouring roots during pullout tests. *Plant Soil* 367:391–406. <https://doi.org/10.1007/s11104-012-1475-1>
- Gray DH, Leiser AT (1982) Biotechnical slope protection and erosion control. Van Nostrand Reinhold Co., New York
- Gurpersaud N, Vanapalli SK, Sivathayalan S (2011) Pull-out capacity of soil nails in unsaturated soils. Toronto, Ontario, Canada
- Gurpersaud N, Vanapalli SK, Sivathayalan S (2013) Semi-empirical method for estimation of pullout capacity of grouted soil nails in saturated and unsaturated soil environments. *J Geotech Geoenviron Eng* 139:1934–1943. [https://doi.org/10.1061/\(ASCE\)GT.1943-5606.0000883](https://doi.org/10.1061/(ASCE)GT.1943-5606.0000883)
- Hales TC, Miniati CF (2017) Soil moisture causes dynamic adjustments to root reinforcement that reduce slope stability. *Earth Surf Proc Land* 42:803–813. <https://doi.org/10.1002/esp.4039>
- Hamid T, Miller G (2009) Shear strength of unsaturated soil interfaces. *Can Geotech J* 46:595–606. <https://doi.org/10.1139/T09-002>
- Han F, Ganju E, Salgado R, Prezzi M (2018) Effects of interface roughness, particle geometry, and gradation on the sand-steel interface friction angle. *J Geotech Geoenviron Eng*. [https://doi.org/10.1061/\(ASCE\)GT.1943-5606.0001990](https://doi.org/10.1061/(ASCE)GT.1943-5606.0001990)
- Hatami K, Esmaili D (2015) Unsaturated soil-woven geotextile interface strength properties from small-scale pullout and interface tests. *Geosynth Int* 22:161–172. <https://doi.org/10.1680/gein.15.00002>
- Hatami K, Khoury C, Miller G (2008) Suction-controlled testing of soil-geotextile interfaces. In: *GeoAmericas 2008, the First Pan American Geosynthetics Conference & Exhibition*. 262–271
- Hubble TCT, Docker BB, Rutherford ID (2010) The role of riparian trees in maintaining riverbank stability: a review of Australian experience and practice. *Ecol Eng* 36:292–304. <https://doi.org/10.1016/j.ecoleng.2009.04.006>
- Hubble TCT, Rutherford ID (2010) Evaluating the relative contributions of vegetation and flooding in controlling channel widening: the case of the Nepean River, southeastern Australia. *Aust J Earth Sci* 57:525–541. <https://doi.org/10.1080/08120099.2010.492910>
- Ji J, Mao Z, Qu W, Zhang Z (2020) Energy-based fibre bundle model algorithms to predict soil reinforcement by roots. *Plant Soil* 446:307–329. <https://doi.org/10.1007/s11104-019-04327-z>
- Kamchoom V (2015) Effects of root geometry and transpiration on slope stability: centrifuge and numerical modelling. Hong Kong University of Science and Technology, Hong Kong
- Kamchoom V, Ng CWW, Leung A (2014) Effects of root geometry and transpiration on pull-out resistance. *Géotechnique Letters* 4:330–336. <https://doi.org/10.1680/geolett.14.00086>
- Khalili N, Khabbaz MH (1998) A unique relationship for χ for the determination of the shear strength of unsaturated soils. *Géotechnique* 48:681–687. <https://doi.org/10.1680/geot.1998.48.5.681>
- Kodikara J (2012) New framework for volumetric constitutive behaviour of compacted unsaturated soils. *Can Geotech J* 49:1227. <https://doi.org/10.1139/t2012-084>
- Kodikara J, Islam T, Wijesooriya S, Burman B, Bui H (2014) On controlling influence of the line of optimums on the compacted

- clayey soil behavior. In: Khalili N, Russell A, Khoshghalb A (eds) *Unsaturated soils: research & applications*. CRC Press, Boca Raton
34. Loades KW, Bengough AG, Bransby MF, Hallett PD (2010) Planting density influence on fibrous root reinforcement of soils. *Ecol Eng* 36:276–284. <https://doi.org/10.1016/j.ecoleng.2009.02.005>
 35. Lu N, Godt JW, Wu DT (2010) A closed-form equation for effective stress in unsaturated soil. *Water Resour Res*. <https://doi.org/10.1029/2009WR008646>
 36. Mahannopkul K, Jotisankasa A (2019) Influences of root concentration and suction on chrysopogon zizanioides reinforcement of soil. *Soils Found*. <https://doi.org/10.1016/j.sandf.2018.12.014>
 37. Masi EB, Segoni S, Tofani V (2021) Root reinforcement in slope stability models: a review. *Geosciences* 11:212. <https://doi.org/10.3390/geosciences11050212>
 38. Meijer GJ (2021) A generic form of fibre bundle models for root reinforcement of soil. *Plant Soil* 468:45–65. <https://doi.org/10.1007/s11104-021-05039-z>
 39. Milligan GWE, Tei K (1998) The pull-out resistance of model soil nails. *Soils Found* 38:179–190. https://doi.org/10.3208/sandf.38.2_179
 40. Mualem Y (1976) A new model for predicting the hydraulic conductivity of unsaturated porous media. 12: 513–522. <https://doi.org/10.1029/WR012i003p00513>
 41. Ng C, Leung A, Ni J (2019) *Plant-soil slope interaction*. CRC Press, Boca Raton
 42. Nilaweera NS, Nutalaya P (1999) Role of tree roots in slope stabilisation. *Bull Eng Geol Env* 57:337–342. <https://doi.org/10.1007/s100640050056>
 43. Öberg AL, Sällfors G (1997) Determination of shear strength parameters of unsaturated silts and sands based on the water retention curve. *Geotech Test J* 20:40–48. <https://doi.org/10.1520/GTJ11419J>
 44. Operstein V, Frydman S (2000) The influence of vegetation on soil strength. *Proc Inst Civil Eng—Ground Improv* 4:81–89. <https://doi.org/10.1680/grim.2000.4.2.81>
 45. Pollen N (2007) Temporal and spatial variability in root reinforcement of streambanks: accounting for soil shear strength and moisture. *CATENA* 69:197–205. <https://doi.org/10.1016/j.catena.2006.05.004>
 46. Pollen N, Simon A (2005) Estimating the mechanical effects of riparian vegetation on stream bank stability using a fiber bundle model. *Water Resour Res*. <https://doi.org/10.1029/2004WR003801>
 47. Rahardjo H, Satyanaga A, D'Amore GAR, Leong E-C (2012) Soil–water characteristic curves of gap-graded soils. *Eng Geol* 125:102–107. <https://doi.org/10.1016/j.enggeo.2011.11.009>
 48. Rahardjo H, Satyanaga A, Wang CL, Wong JLH, Han LV (2018) Effects of unsaturated properties on stability of slope covered with *Caesalpinia crista* in Singapore. *Environ Geotech* 7:393–403. <https://doi.org/10.1680/jenge.17.00031>
 49. Satyanaga A, Rahardjo H, Zhai Q (2017) Estimation of unimodal water characteristic curve for gap-graded soil. *Soils Found* 57:789–801. <https://doi.org/10.1016/j.sandf.2017.08.009>
 50. Schwarz M, Cohen D, Or D (2011) Pullout tests of root analogs and natural root bundles in soil: experiments and modeling. *J Geophys Res Earth Surf*. <https://doi.org/10.1029/2010JF001753>
 51. Schwarz M, Giadrossich F, Cohen D (2013) Modeling root reinforcement using a root-failure Weibull survival function. *Hydrol Earth Syst Sci* 17:4367–4377. <https://doi.org/10.5194/hess-17-4367-2013>
 52. Schwarz M, Lehmann P, Or D (2010) Quantifying lateral root reinforcement in steep slopes—From a bundle of roots to tree stand. *Earth Surf Proc Land* 35:354–367. <https://doi.org/10.1002/esp.1927>
 53. Sheng D, Fredlund D, Gens A (2008) A new modeling approach to unsaturated soils using independent stress variables. *Can Geotech J* 45:511–534. <https://doi.org/10.1139/T07-112>
 54. Galpathage SG (2017) *Experimental and numerical study of root reinforcement and suction in soil stabilisation*. University of Wollongong, Wollongong
 55. Simon A, Pollen N (2004) Hydrologic controls of riparian vegetation on the geotechnical stability of streambanks: experimental results. *American Society of Civil Engineers, Reston*, pp 1–12
 56. Skempton AW, Delory FA (1957) *Stability of natural slopes in london clay*. Thomas Telford Publishing, London, pp 70–73
 57. Su L-J, Chan T, Shiu YK, Cheung T, Yin J-H (2008) Influence of degree of saturation on soil nail pull-out resistance in compacted completely decomposed granite fill. *Can Geotech J* 44:1314–1328. <https://doi.org/10.1139/T07-056>
 58. Subba Rao KS, Allam MM, Robinson RG (1996) A note on the choice of interfacial friction angle.
 59. Świątała BM, Wu W (2018) Numerical modelling of rainfall-induced instability of vegetated slopes. *Géotechnique* 68:481–491. <https://doi.org/10.1680/jgeot.16.P.176>
 60. Terzaghi K (1943) *Arching in ideal soils*. *Theoretical Soil Mechanics*. Wiley, New York, pp 66–76
 61. Terzaghi K, Peck RB (1948) *Soil mechanics in engineering practice*. John Wiley and Sons, New York
 62. Thomas R, Pollen-Bankhead N (2010) Modeling root-reinforcement with a fiber-bundle model and Monte Carlo simulation. *Ecol Eng* 36:47–61. <https://doi.org/10.1016/j.ecoleng.2009.09.008>
 63. Van Genuchten M (1980) A closed-form equation for predicting the hydraulic conductivity of unsaturated soils I. *Soil Sci Soc Am J*. <https://doi.org/10.2136/sssaj1980.03615995004400050002x>
 64. Vanapalli S, Fredlund D (2000) Comparison of different procedures to predict unsaturated soil shear strength. *Geotech Spec Publ*. [https://doi.org/10.1061/40510\(287\)13](https://doi.org/10.1061/40510(287)13)
 65. Vanapalli S, Fredlund D, Pufahl DE, Clifton AW (1996) Model for the prediction of shear strength with respect to soil suction. *Canadian Geotech J—can Geotech J* 33:379–392. <https://doi.org/10.1139/96-060>
 66. Vanapalli S, Taylan Z (2011) *Estimation of the shaft capacity of model piles in a compacted fine-grained unsaturated soil*. Toronto, Ontario, Canada
 67. Vanapalli SK, Eigenbrod KD, Taylan ZN, Catana C, Oh WT, Garven E (2010) A technique for estimating the shaft resistance of test piles in unsaturated soils. In: Gens A (ed) *Unsaturated soils, two volume set*. CRC Press, Boca Raton
 68. Waldron LJ (1977) The shear resistance of root-permeated homogeneous and stratified soil. *Soil Sci Soc Am J* 41:843–849. <https://doi.org/10.2136/sssaj1977.03615995004100050005x>
 69. Wang H, He Y, Shang Z, Han C, Wang Y (2018) Model test of the reinforcement of surface soil by plant roots under the influence of precipitation. *Adv Mater Sci Eng* 2018:3625053. <https://doi.org/10.1155/2018/3625053>
 70. Wu TH, Bettadapura DP, Beal PE (1988) A statistical model of root geometry. *For Sci* 34:980–997. <https://doi.org/10.1093/for-estscience/34.4.980>
 71. Wu TH, McKinnell WP III, Swanston DN (1979) Strength of tree roots and landslides on Prince of Wales Island, Alaska. *Can Geotech J* 16:19–33. <https://doi.org/10.1139/t79-003>

72. Wu TH, McOmber RM, Erb RT, Beal PE (1988) Study of soil-root interaction. *J Geotech Eng* 114:1351–1375. [https://doi.org/10.1061/\(ASCE\)0733-9410\(1988\)114:12\(1351\)](https://doi.org/10.1061/(ASCE)0733-9410(1988)114:12(1351))
73. Ye X, Wang S, Wang Q, Sloan S, Sheng D (2019) The influence of the degree of saturation on compaction-grouted soil nails in sand. *Acta Geotech*. <https://doi.org/10.1007/s11440-018-0706-x>
74. Yusoff NA, Fauzi MFM, Abdullah F (2016) The study of soil-roots strength performance by using *Pennisetum setaceum* grass. *MATEC Web of Conf* 47:03021. <https://doi.org/10.1051/matec/conf/20164703021>
75. Zhang C, Liu Y, Liu P, Jiang J, Yang Q (2020) Untangling the influence of soil moisture on root pullout property of alfafa plant. *J Arid Land*. <https://doi.org/10.1007/s40333-020-0017-6>

Publisher's Note Springer Nature remains neutral with regard to jurisdictional claims in published maps and institutional affiliations.